Chapter 1

COMPTONIZATION, REFLECTION AND NOISE IN BLACK HOLE BINARIES

M.Gilfanov[1,2], E.Churazov[1,2], M.Revnivtsev[2,1]
[1] *Max-Planck-Institute für Astrophysik, Karl-Schwarzschild-Str. 1, D-85740 Garching, Germany*
[2] *Space Research Institute, Profsoyuznaya 84/32, 117810 Moscow, Russia*

Abstract

Based on the analysis of a large sample of RXTE/PCA observations of several black hole binaries in the low spectral state we show that a correlation exists between the spectral parameters and characteristic noise frequency. In particular, the amplitude of reflection increases and the slope of Comptonized radiation steepens as the noise frequency increases. We consider implications of these results on the accretion flow models and discuss a possible observational test aimed to discriminate between different geometries of the accretion flow.

Keywords: accretion, accretion disks – black hole physics – stars: binaries: general – stars: individual: Cygnus X-1, GX339-4, GS1354-644 – X-rays: general – X-rays: stars

Comptonization of soft seed photons in a hot, optically thin electron cloud near the compact object is thought to produce the hard X–ray radiation in the low spectral state of accreting black holes (Sunyaev & Truemper 1979, Sunyaev & Titarchuk 1980). The slope of the Comptonized spectrum is governed by the ratio of the energy deposited into the electrons and the influx of the soft radiation into the Comptonization region; the lower the ratio the steeper the Comptonized spectrum (e.g. Sunyaev & Titarchuk 1989, Haardt & Maraschi 1993, Gilfanov et al. 1995).

Reflection of the Comptonized radiation from neutral or partially ionized matter, presumably the optically thick accretion disk, leads to appearance of characteristic features in the spectra of X–ray binaries (Fig.1.1). The main

* To appear in the Proceedings of the 5th CAS/MPG Workshop on High Energy Astrophysics

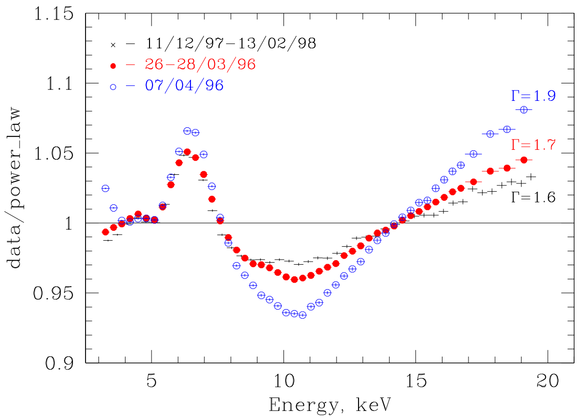

Figure 1.1 The counts spectra of Cyg X–1 at different epoch plotted as a ratio to a power law model. The power law photon index is indicated against each spectrum.

signatures of the emission reflected from cold neutral medium are well known – the fluorescent K_α line of iron at 6.4 keV, iron K-edge at 7.1 keV and a broad hump above $\sim 20-30$ keV (Basko, Sunyaev & Titarchuk 1974, George & Fabian 1991). The exact shape of these spectral features in the X-ray binaries depends on the ionization state of the reflecting medium (Ross, Fabian & Young 1999) and might be modified by the strong gravity effects and intrinsic motions in the reflector (e.g. Fabian et al., 1989). The amplitude of the reflection signatures depends primarily on the ionization state and on the solid angle of the reflector as seen from the source of the primary radiation.

Based on the analysis of a large sample of Seyfert AGNs and several X–ray binaries Zdziarski, Lubinski & Smith 1999 (see also Zdziarski 2000) found a correlation between the amplitude of reflection and the slope of the underlying power law. They concluded that the existence of such a correlation implies a dominant role of the reflecting medium as the source of seed photons to the Comptonization region.

The power density spectra of the black hole binaries in the low state (see van der Klis 1995 for a review) plotted in the units of frequency×power usually appear as a superposition of two or more rather broad humps containing most of the power of aperiodic variations below several tens Hz (Fig.1.2). These humps define several characteristic noise frequencies of which the lowest usually corresponds to the break frequency ν_{br} of the band limited noise component. Although a number of theoretical models was proposed to explain the power spectra of X–ray binaries (e.g. Alpar et al. 1992, Stella Vietri & Morsink 1999), the nature of the characteristic noise frequencies is still unclear. Despite the fact that the characteristic noise frequencies vary from source to source and

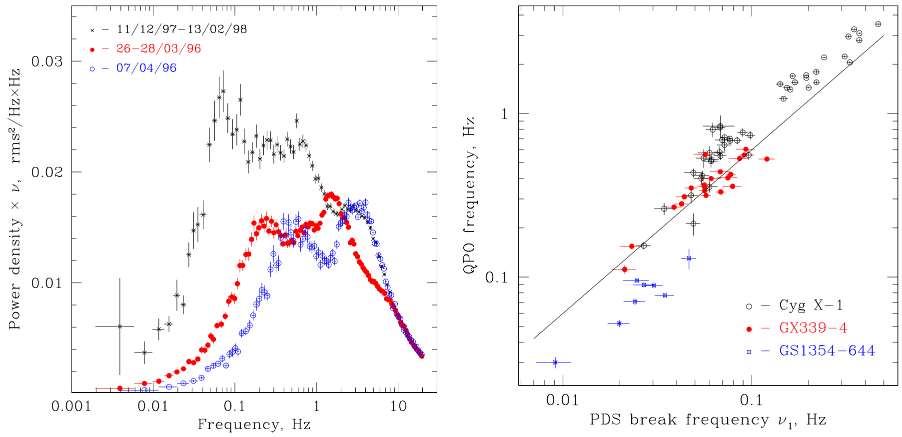

Figure 1.2 *Left:* The power density spectra of Cyg X–1 at different epoch. The power density spectra are plotted as frequency × (power density), i.e. in units of Hz × rms^2/Hz. The observations and the symbols are the same as in Fig.1.1 *Right:* The relation between the QPO centroid frequency and the break frequency of the band limited noise for Cyg X-1, GX339–4 and GS1354–644. The solid line is $f_{qpo} = 6 \times f_{br}$.

from epoch to epoch, they are correlated with the break frequency of the band limited noise (Fig.1.2, Wijnands & van der Klis 1999).

Gilfanov, Churazov & Revnivtsev 1999 showed that a tight correlation exists between the characteristic noise frequencies and the spectral parameters. Based on RXTE/PCA observations of Cyg X–1 from 1996–1998 they found that the amplitude of reflection increases and the spectrum of primary radiation steepens as the noise frequency increases. An identical behavior was found for another black hole candidate, GX339-4, by Revnivtsev, Gilfanov & Churazov 2000. Interpreting these correlations Gilfanov, Churazov & Revnivtsev 1999 suggested that increase of the noise frequency might be caused by the shift of the inner boundary of the optically thick accretion disk towards the compact object. The related increase of the solid angle, subtended by the disk, and of the influx of the soft photons to the Comptonization region lead to an increase of the amount of reflection and steepening of the Comptonized spectrum.

Below we investigate further the relation between the spectral parameters and characteristic noise frequencies based on a larger sample of objects and observations and discuss implications of these results on the geometry of the accretion flow in the low spectral state of black hole binaries.

1. THE DATA

Observations and data reduction. The results presented below are based on the publicly available data of Cyg X–1, GX339–4 and GS1354–644 observations with the Proportional Counter Array aboard the Rossi X-ray Timing Explorer (Brandt Rotschild & Swank 1996) from 1996–1998 during the low (hard) spectral state of the sources. In total our sample included ≈ 60 observations of these sources. The energy and power density spectra were averaged for each individual observation. The energy spectra were extracted from the "Standard Mode 2" data and ARF and RMF were constructed using standard RXTE FTOOLS v.4.2 tasks. The "VLE" and "Q6" models were used for the background calculation with the preference being given to the "VLE" model when possible. A uniform systematic error of 0.5% was added quadratically to the statistical error in each energy channel. The power spectra were calculated in the 2–16 keV energy band and in the $\approx 0.005 - 32$ Hz frequency range following the standard X–ray timing technique and normalized to units of squared fractional rms.

The spectral model. The energy spectra were fit with a model consisting of a power law with a superimposed reflected continuum (pexrav model in XSPEC, Magdziarz & Zdziarski 1995) and an intrinsically narrow line at $\sim 6.4 - 6.7$ keV. The centroid energy of the line was a free parameter of the fit. For all sources the binary system inclination was fixed at $i = 50$ degrees, the iron abundance – at the solar value of $A_{\rm Fe} = 3.3 \cdot 10^{-5}$ and the low energy absorption – at $N_{\rm H} = 6 \cdot 10^{21}$ cm^{-2}. The effects of ionization were not included. In order to approximately include in the model the smearing of the reflection features due to motion in the accretion flow the reflection continuum and line were convolved with a Gaussian, which width was a free parameter of the fit. The spectra were fitted in the 4–20 keV energy range. This spectral model is identical to that applied by Gilfanov, Churazov & Revnivtsev 1999 to the Cyg X-1 data, except that in the present analysis we let the line centroid energy be a free parameter of the fit. Strength of the reflected component is characterized in the pexrav model by the reflection scaling factor R, which approximately measures the solid angle subtended by the reflecting media as seen from the source of the primary radiation, $R \approx \Omega_{refl}/2\pi$, so that $R = 1$ for an isotropic point source above an infinite optically thick slab.

The spectral model is obviously oversimplified. Moreover, several important parameters, such as the binary system inclination angle and the iron abundance were fixed at fiducial values. Therefore the best fit values do not necessarily represent the exact values of the physically interesting parameters. Particularly subject to the uncertainties due to the choice of the spectral model is the reflection scaling factor $R \sim \Omega/2\pi$. This might explain the values of R

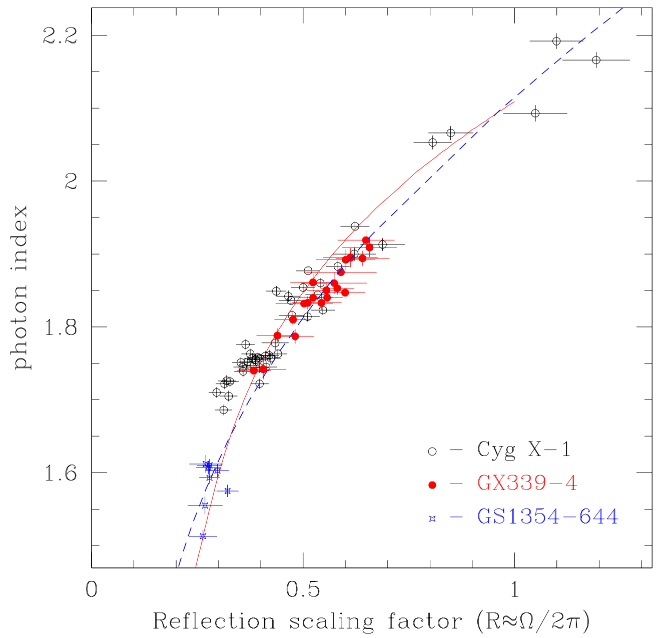

Figure 1.3 The best fit values of the photon index of the underlying power law plotted vs. reflection scaling factor for Cyg X-1, GX339–4 and GS1354–644. The solid line shows the dependence $\Gamma(R)$ of the photon index of the Comptonized radiation Γ on the strength of the reflected emission R expected in the disk–spheroid model assuming the disk albedo $a = 0.1$, Thomson optical depth of the cloud $\tau_T = 1$ and the ratio of the temperature of the seed photons to the electron temperature $T_{bb}/T_e = 10^{-4}$. The dashed line shows $\Gamma(R)$ dependence expected in the plasma ejection model (Beloborodov 1999) for $a = 0.15$, $\tau_T = 1$, $T_{bb}/T_e = 3 \cdot 10^{-3}$ and $\mu_s = 0.3$.

exceeding unity obtained for some of the spectra. However, as was shown by Gilfanov, Churazov & Revnivtsev 1999 the model correctly ranks the spectra according to the strength of the reflected component and the slope of the underlying power law.

Power spectra approximation. The power density spectra in units of rms^2/Hz were fit in the 0.005–15 Hz frequency range with a model, consisting of two broken constant components and a Lorentzian profile $P_\nu = \frac{P_0}{1+(2(\nu-\nu_0)/\Delta\nu)^2}$. We use centroid frequency of the Lorentzian profile as a characteristic noise frequency. Its dependence on the break frequency of the band limited noise (the first broken constant component in the model) is shown in Fig.1.2.

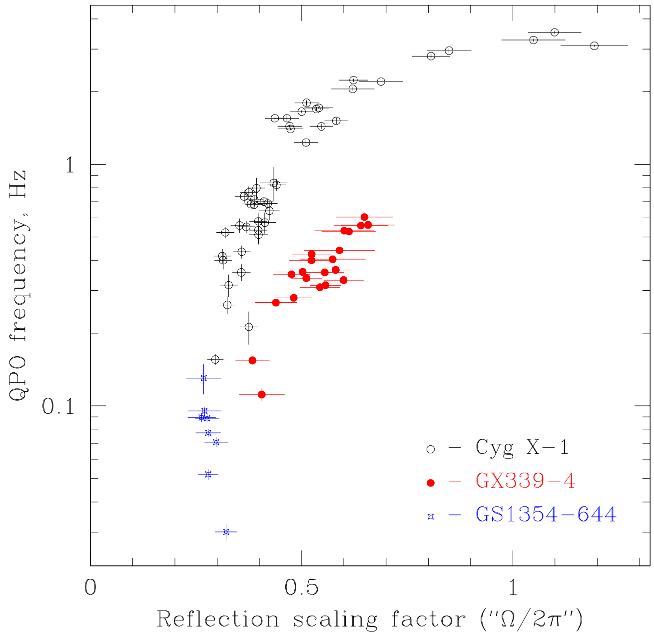

Figure 1.4 The QPO centroid frequency plotted vs. reflection scaling factor for the same set of observations of Cyg X-1, GX339–4 and GS1354–644 as in Fig.1.3 and 1.6.

Correlation between the spectral parameters and the noise frequency. The results of the energy and power spectra approximation are presented in Fig. 1.3 and 1.4 showing dependence of the slope of the primary emission and characteristic noise frequency on the amplitude of the reflected component. The noise frequency and the spectral parameters are clearly correlated. An increase of the amplitude of the reflected component is accompanied with a steepening of the spectrum of the primary emission and an increase of the noise frequency.

2. DISCUSSION

Slope of the Comptonized spectrum and reflection. The photon index Γ of the Comptonized radiation is governed by the Compton amplification factor A which equals to the ratio of the energy deposited into the hot electrons to the influx of the soft seed photons to the Comptonization region. The concrete shape of the $\Gamma(A)$ relation depends on the ratio T_{bb}/T_e of the temperatures of the seed photons and the electrons, the Thomson optical depth and the geometry. In the simplest although not unique scenario the correlation between the amplitude of the reflected component R and the slope of the primary radiation Γ (Fig.1.3)

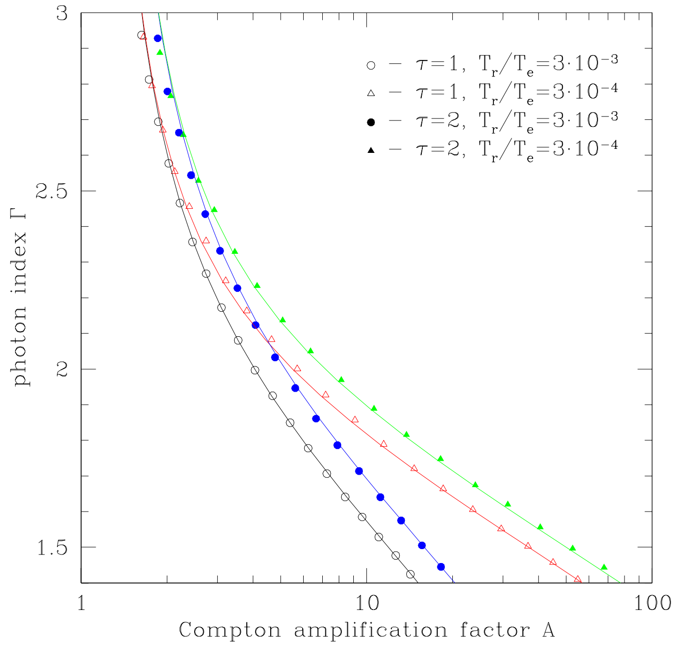

Figure 1.5 Relation between the Compton amplification factor and photon index of Comptonized radiation for an isotropic point source of the soft seed photons with temperature T_r in the center of a uniform sphere with electron temperature T_e and Thomson optical depth $\tau_T = 1$ (hollow symbols) and $\tau_T = 2$ (solid symbols). The symbols are a result of the Monte-Carlo calculations, the solid curves were calculated according to the formula given in the text.

could be understood assuming that there is a positive correlation between the solid angle subtended by the reflecting media, Ω_{refl}, and the influx of the soft photons to the Comptonization region (Zdziarski, Lubinski & Smith 1999). Existence of such correlation is a strong argument in favor the reflecting media being the primary source of the soft seed photons to the Comptonization region. In the absence of strong beaming effects a correlation between Ω_{refl} and the seed photons flux should be expected since an increase of the solid angle of the disk seen by the hot electrons ($= \Omega_{refl}$) should generally lead to the increase of the fraction of the disk emission reaching the Comptonization region.

In order to demonstrate that such geometrical effects can explain the observed dependence $\Gamma(R)$ we consider two idealized models having different cause of change of the Ω_{refl}. In the first, disk-spheroid model, an optically thin uniform hot sphere with radius R_{sph} is surrounded with an optically thick cold disk with an inner radius R_{disk} (e.g. Poutanen Krolik & Ryde 1997), the Ω_{refl} depending on the ratio R_{disk}/R_{sph}. Propagation of the disk towards/inwards the hot sphere (decrease of R_{disk}/R_{sph}) leads to an increase of the reflection scaling factor, a decrease of the the Compton amplification factor A and a steepening of the Comptonized spectrum. In such context the model was first studied by Zdziarski, Lubinski & Smith 1999 and we used their results to calculate the relation between the reflection scaling factor R and the Compton amplification A. In the second, plasma ejection model, value of the Ω_{refl} is defined by the intrinsic properties of the emitting hot plasma, particularly by its bulk motion with mildly relativistic velocity towards or away from the disk, which itself remains unchanged (Beloborodov 1999). In the case of an infinite disk, values of reflection below and above unity correspond to the hot plasma moving respectively away and towards the disk. Both models predict relation between reflection R and Compton amplification factor A which can be translated to $\Gamma(R)$ given a dependence $\Gamma(A)$ of the photon index of Comptonized spectrum on the amplification factor. The latter was approximated by:

$$A = (1 - e^{-\tau_T}) \cdot \frac{1-\Gamma}{2-\Gamma} \cdot \frac{\left(\frac{T_e}{T_{bb}}\right)^{2-\Gamma} - 1}{\left(\frac{T_e}{T_{bb}}\right)^{1-\Gamma} - 1} + e^{-\tau_T}$$

This formula is based on a representation of the Comptonized spectrum by a power law in the energy range $3kT_{bb} - 3kT_e$ and agrees with the results of the Monte-Carlo calculations with reasonable accuracy for optical depth $\tau_T \sim 1$ and $T_{bb}/T_e \sim 10^{-5} - 10^{-3}$ (Fig.1.5).

The expected $\Gamma(R)$ relations are shown in Fig.1.3. With a proper tuning of the parameters both models can reproduce the observed shape of the $\Gamma(R)$ dependence and in this respect are virtually indistinguishable. The observed range of the reflection $R \sim 0.3-1$ and the slope $\Gamma \sim 1.5-2.2$ can be explained assuming variation of the disk radius in from $R_{disk} \sim R_{sph}$ to $R_{disk} \sim 0$ in the disk-spheroid model or variation of the bulk motion velocity from $v \sim 0.4c$ away from the disk to $v \sim 0$ in the plasma ejection model. Finally, it should be emphasized that these idealized models do not include a number of important effects which might affect the particular shape of the $\Gamma(R)$ dependence.

Relativistic smearing and reflection. The spectrum of emission, reflected from a Keplerian accretion disk is expected to be modified by special and general relativity effects (e.g. Fabian et al., 1989). If increase of the reflection is caused by a shift of the inner boundary of the accretion disk closer to the compact object, a correlation between the reflection and relativistic smearing should be expected. Such a correlation is a generic prediction of the model and might be used to discriminate between different assumptions about geometry of the accretion flow. The energy resolution of RXTE/PCA is not adequate to study relativistic smearing of the reflection features with sufficient degree of confidence. However, the data shown in Fig.1.6 might present an evidence in favor of correlated behavior of the reflection and relativistic smearing. If

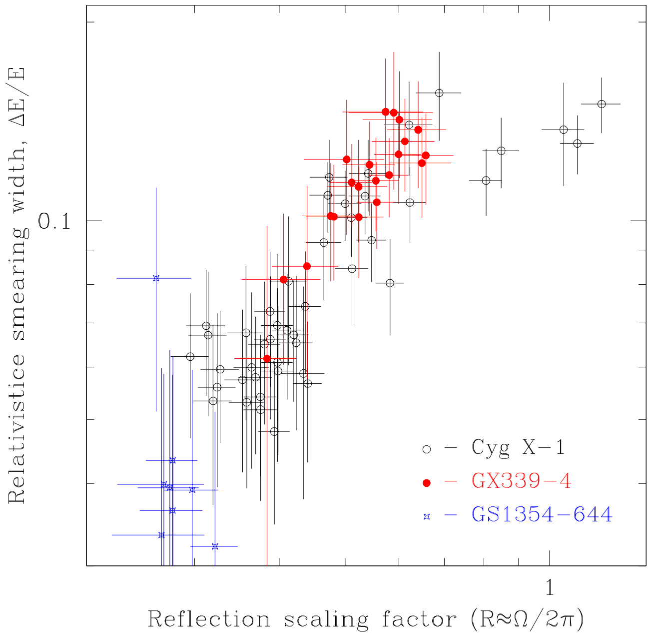

Figure 1.6 The best fit value of the relative width of the relativistic smearing of the reflection features plotted vs. reflection scaling factor for Cyg X-1, GX339–4 and GS1354–644.

confirmed, it would prove that the spectral and timing properties in the low state of the black hole binaries are defined mainly by the position of the inner boundary of the optically thick accretion disk.

3. CONCLUSIONS

In the low spectral state of black hole candidates the amplitude of reflection R, slope of the Comptonized radiation Γ and characteristic noise frequency change in a correlated way. The correlation between the slope and reflection indicates that the accretion disk is the primary source of the soft seed photons for Comptonization. We considered two idealized models, the disk–spheroid and plasma ejection model, and showed that with appropriate tuning of the parameters either model can explain the observed $\Gamma(R)$ dependence. The RXTE data also hints at a correlated change of the width of relativistic smearing of the reflection features. If confirmed by observations with better energy resolution, this correlation may help to distinguish between different geometries of the accretion flow.

Acknowledgments

This research has made use of data obtained through the High Energy Astrophysics Science Archive Research Center Online Service, provided by the NASA/Goddard Space Flight Center. The work was done in the context of the research network "Accretion onto black holes, compact objects and protostars" (TMR Grant ERB-FMRX-CT98-0195 of the European Commission). M.Revnivtsev acknowledges hospitality of the Max–Planck Institute for Astrophysics and a partial support by RBRF grant 96–15–96343 and INTAS grant 93–3364–ext.

References

Alpar M. A., Hasinger G., Shaham J., Yancopoulos S., 1992, A&A 257, 627

Basko M., Sunyaev R., Titarchuk L., 1974, A&A 31, 249

Beloborodov, A. M. 1999, ApJ, 510, L123

Brandt, H., Rotschild, R. & Swank, J. 1996, Memorie della Societa Astronomica Italiana, 67, 593

George I.M., Fabian A.C., 1991, MNRAS 249, 352

Gilfanov M., Churazov E., Sunyaev R. et al., 1995, in: The Lives of the Neutron Stars. Proceedings of the NATO ASI, eds. M.A. Alpar, U. Kiziloglu, J. van Paradijs; Kluwer Academic, p.331

Gilfanov M., Churazov E., Revnivtsev M., 1999 A&A, 352, 182

Haardt F., Maraschi L., 1993, ApJ 413, 507

Magdziarz, P. & Zdziarski, A. A. 1995, MNRAS, 273, 837

Poutanen, J. , Krolik, J. H. & Ryde, F. 1997, MNRAS, 292, L21

Revnivtsev M., Gilfanov M., Churazov E., 2000, A&A Letters, submitted

Ross, R. R., Fabian, A. C. & Young, A. J. 1999, MNRAS, 306, 461

Stella, L. , Vietri, M. & Morsink, S. M. 1999, ApJ, 524, L63

Sunyaev R., Truemper J. 1979, Nature 279, 506

Sunyaev R., Titarchuk L., 1980, A&A 86, 121

Sunyaev R., Titarchuk L., 1989, in Proceedings of “23rd ESLAB Symposium”, ESA SP-296, Bologna, Italy, eds. J.Hunt, B.Battrick, v.1, p.627

van der Klis M., 1995, in: X–ray Binaries, eds. Lewin W., van Paradijs J., van den Heuvel E.P.J.; Cambridge Univ.Press, p.252

Wijnands R., van der Klis M., 1999, ApJ 514, 939

Zdziarski A.A., Lubinski P., Smith D., 1999, MNRAS 303, L11

Zdziarski A.A., in: Highly Energetic Physical Processes and Mechanisms for Emission from Astrophysical Plasmas. IAU Symp., Vol. 195, 2000, Eds: P.C.H.Martens & S.Tsuruta